

# Minimum Energy Diagrams for Multieffect Distillation Arrangements

Hilde K. Engelién and Sigurd Skogestad

Dept. of Chemical Engineering, Norwegian University of Science and Technology (NTNU), 7491 Trondheim, Norway

DOI 10.1002/aic.10453

Published online April 25, 2005 in Wiley InterScience (www.interscience.wiley.com).

*The minimum energy requirements of six different heat-integrated multieffect and three nonintegrated distillation arrangements for separating a ternary mixture have been considered. The focus is on a heat-integrated complex distillation configuration, called a multieffect prefractionator arrangement. The comparison of the different arrangements is based on the minimum vapor flow rates at infinite number of stages, which are easily visualized and compared in a  $V_{min}$  diagram. This tool can be used as a basis for screening and the best arrangement(s) can be studied further using more rigorous simulation methods.* © 2005 American Institute of Chemical Engineers *AIChE J*, 51: 1714–1725, 2005

## Introduction

In the chemical industries, the task of separation is a very energy consuming process, where distillation is the process most widely used for fluid separations. Distillation columns are used for about 95% of liquid separations and the energy use from this process accounts for an estimated 3% of the world energy consumption.<sup>1</sup> With rising energy awareness and growing environmental concerns there is a need to reduce the energy use in industry. For the distillation process, because it is such a high-energy consumer, any energy savings should have an impact on the overall plant energy consumption.

The use of heat integration combined with complex configurations for distillation columns holds a great promise of energy savings up to about 70%. In addition to saving energy, accompanied by reduced environmental impact and site utility costs, there is also a possibility for reduction in capital costs. There are a number of different methods or designs that can be applied to save energy in distillation, such as integration of distillation columns with the background process, heat pumps, multieffect distillation, and complex arrangements such as prefractionators or thermally coupled columns (Petlyuk columns). Deciding which heat-integrated arrangement to use is not a

straightforward task, given that the best arrangement is substantially dependent on the given separation task and the background process.

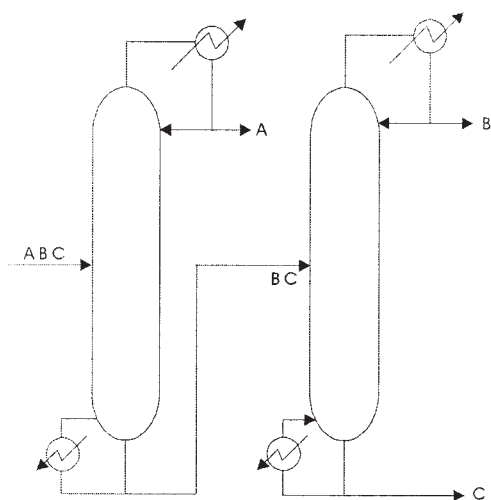
The study of so-called multieffect distillation systems is described in this article. Multieffect integration is achieved for two or more distillation columns by running one of the columns at a higher pressure and integrating the condenser of this high-pressure (HP) column with the reboiler of the low-pressure (LP) column. The objective of this paper is to present a simple graphical method for obtaining the energy usage and to compare the energy savings with the nonintegrated arrangements shown in Figure 1.

For the multieffect systems there are two modes of integration: forward integration, where the heat integration is in the direction of the mass flow; and backward integration, where the integration is in the opposite direction of the mass flow. The arrangements studied are shown in Figures 2–4. Herein the focus is on the multieffect integrated prefractionator arrangement (Figure 4), which has been shown by several authors, for example, Cheng and Luyben<sup>2</sup> and Emtir et al.,<sup>3</sup> to have high energy savings, compared with that of other distillation arrangements.

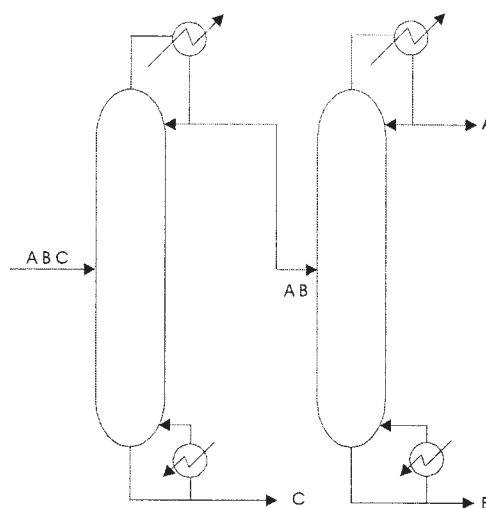
An easy form of comparison for energy consumption is the *minimum vapor flow rate*, which is often expressed by simple shortcut equations. Such equations are given for different integrated multieffect arrangements by Rév et al.<sup>4</sup> Relationships for the prefractionator can be found in Carlberg and Westerbergh.<sup>5</sup>

Correspondence concerning this article should be addressed to S. Skogestad at skoge@chemeng.ntnu.no.

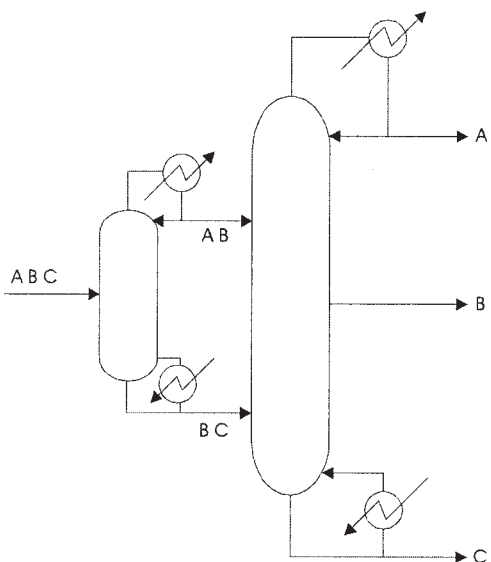
a) Direct split (DS) arrangement



b) Indirect split (IS) arrangement



c) Prefractionator arrangement



d) Petlyuk arrangement

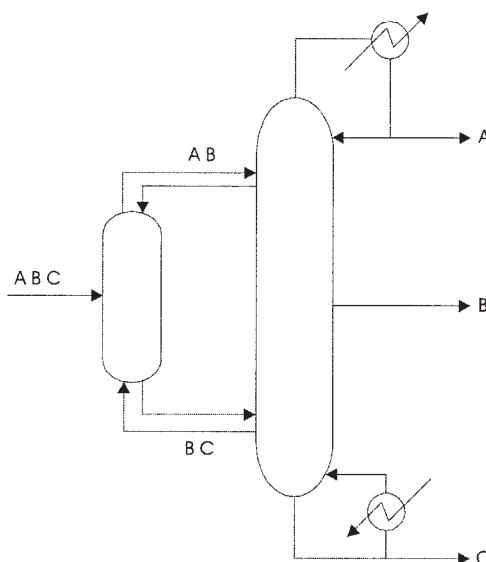
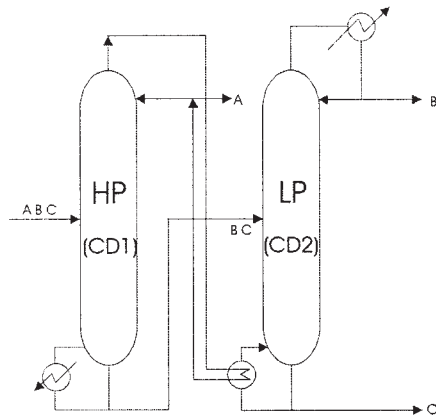


Figure 1. Non-heat-integrated schemes for separating a ternary mixture (ABC).

A visual representation of the minimum vapor flow rate of the fully thermally coupled (Petlyuk) arrangement has been presented by Halvorsen,<sup>6</sup> Fidkowski,<sup>7</sup> and Christiansen.<sup>8</sup> In these diagrams the vapor flow rate is plotted against the distillate/feed ratio in the prefractionator column. Defining the feed composition and the relative volatility of the components being separated, the diagram can be drawn by simply plotting five points (see Figure 5). The diagram can be used to find the minimum vapor flow rate for the Petlyuk column, as well as the recovery for the preferred split.

As shown herein, the  $V_{\min}$  diagram developed for the Petlyuk columns can be used for multieffect heat-integrated systems if it is modified to also include the minimum vapor flow rate for a sharp binary A/B and B/C split. The diagram can then be used to find the minimum vapor flow rate for all six multieffect columns in Figures 2–4. Also it can be used to obtain and to find further information about the multieffect heat-integrated prefractionator arrangement, such as the optimal recovery of the middle component, if the columns are balanced and compare the savings from the integrated arrangement with the Petlyuk arrangement.

a) Direct split with forward integration  
(DSF)



b) Direct split with backward integration  
(DSB)

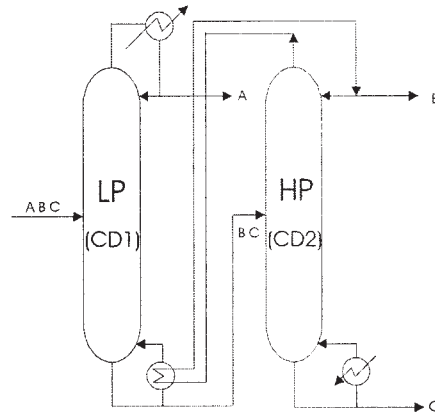


Figure 2. Multieffect direct split arrangements.

### Multieffect Arrangements

Figure 1 shows four non-heat-integrated schemes for separation of a ternary mixture (ABC): (1) a direct split (DS) arrangement, (2) an indirect split (IS) arrangement, (3) a prefractionator (P) arrangement, and (4) a directly coupled prefractionator (Petlyuk) arrangement. In the DS arrangement (Figure 1a) the lightest component (A) is split off in the first column. For the IS arrangement (Figure 1b) the heaviest component (C) is split off in the first column. For the prefractionator and Petlyuk arrangement (Figures 1c and 1d) the split in the first column is between the lightest (A) and the heaviest (C) component, with the middle component (B) being distributed between the two products.

The three first arrangements shown in Figure 1 can be heat integrated in a multieffect fashion by running one column at a higher pressure and then combining the condenser of the HP column with the reboiler of the LP column. Each of these can

be integrated in a *forward* or *backward* fashion, giving us six different schemes to consider:

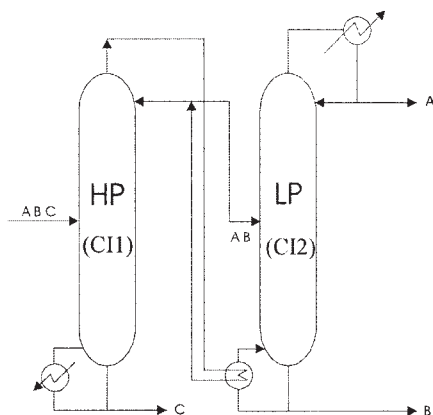
(1) *Direct split columns.* Two possible configurations are possible for the direct split: a forward integration (DSF) as in Figure 2a and a backward integration (DSB) as in Figure 2b.

(2) *Indirect split columns.* Two possible configurations are possible for the indirect split: a forward integration (ISF) as in Figure 3a and a backward integration (ISB) as in Figure 3b.

(3) *Prefractionator arrangement.* The two column options considered are a forward split (PF) (see Figure 4a) and a backward split (PB) (see Figure 4b).

It should be noted that an additional scheme is available for the prefractionator design if the separation is carried out in three columns with three pressure levels. This arrangement, called a *dual* scheme, has not been considered here because the energy consumption is the same as that for the two-column multieffect prefractionator arrangement and be-

a) Indirect split with forward integration  
(ISF)



b) Indirect split with backward integration  
(ISB)

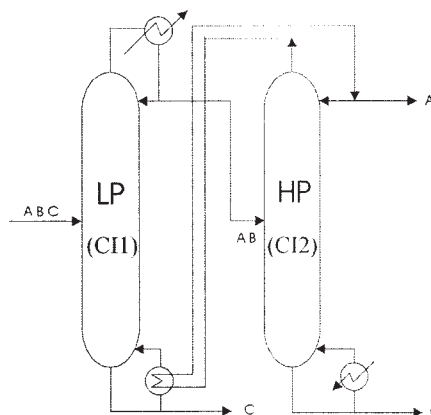


Figure 3. Multieffect indirect split arrangements.

a) Prefractionator with forward integration (PF)      b) Prefractionator with backward integration (PB)

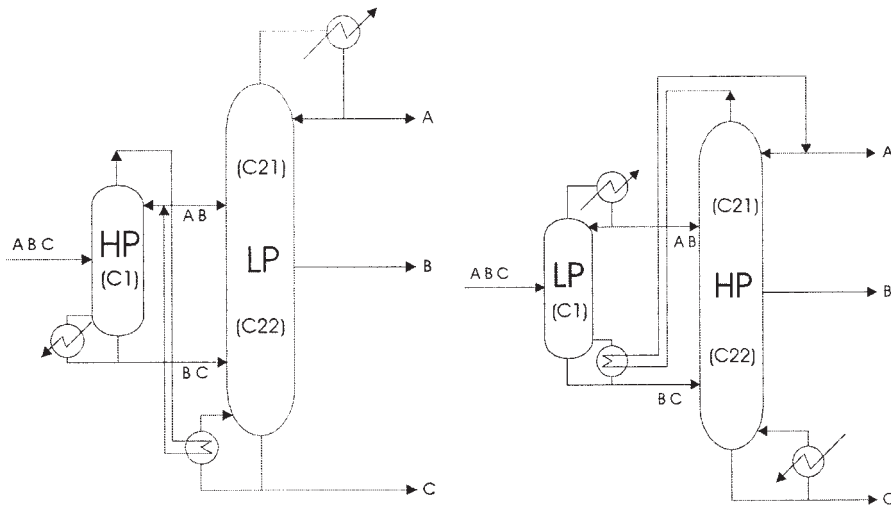


Figure 4. Multieffect prefractionator arrangements.

cause this three-column arrangement would result in a higher capital cost.

In all cases the products and flows between the integrated columns are assumed to be liquid. This may seem nonoptimal, but because of the multieffect integration there is no advantage in using vapor flows between these columns. This follows because (1) it is better to supply the vapor in the reboiler (ISF, PF) and (2) it is not economical to compress vapor going from the LP to the HP column (ISB, PB).

### Minimum Vapor Flow (Energy Requirements)

In the following we consider ideal mixtures where we can assume constant relative volatility ( $\alpha_i$  constant) for the vapor

liquid equilibrium and constant molar flows for the energy balance. For all shortcut equations sharp splits are assumed and the vapor flow rate ( $V$ ) is the bottom flow rate, unless otherwise stated.

The minimum energy required is obtained using column sections with an infinite number of stages, which provides a useful target for distillation where one can easily obtain within 10% of this target with a reasonable number of stages.

The feed data required for the shortcut calculations are the flow rate ( $F$ ) and the composition ( $z$ ), defined herein as  $[z_A \ z_B \ z_C]$  for the ternary mixture ABC. In addition we require the relative volatilities between the components  $[\alpha_{AC} \ \alpha_{BC} \ \alpha_{CC}]$ , which are referenced to the heaviest component (C), so  $\alpha_{CC} = 1$ . Also needed is the feed liquid fraction  $q$ , where  $q = 1$  is liquid feed and  $q = 0$  is vapor feed.

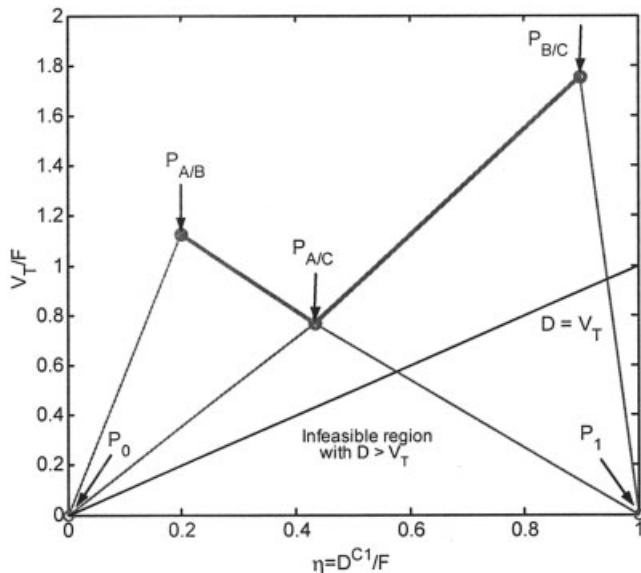


Figure 5.  $V_{\min}$  diagram for ternary separation.

### Minimum vapor flow expressions (Underwood and King)

For a multicomponent mixture the vapor flow rate for a given separation can be calculated using Underwood's equations.<sup>9</sup> The minimum vapor flow rate ( $V_{\min}$ ) at the top of the column is given as

$$V_{T,\min} = \sum_{i=1}^{N_c} \frac{\alpha_{iH} x_{i,D} D}{\alpha_{iH} - \theta} \quad (1)$$

where  $x_{i,D}$  is the distillate composition of component  $i$ ,  $\alpha_{iH}$  is the relative volatility with respect to the heaviest component  $H$ , and  $\theta$  is the Underwood root. For a mixture of  $N_c$  components the  $(N_c - 1)$  Underwood roots  $\theta$  are found as the solution of the so-called feed equation

$$(1 - q) = \sum \frac{\alpha_{iH} z_i}{\alpha_{iH} - \theta} \quad (2)$$

Here  $z_i$  is the feed composition of component  $i$  and  $q$  is the liquid fraction of the feed. The roots lie between the values of neighboring relative volatilities so:  $\alpha_{1H} > \theta_1 > \alpha_{2H} > \theta_2 > \alpha_{3H} > \theta_3 > \dots > \alpha_{N_c-1H} > \theta_{N_c}$ . Equation 2 applies for minimum reflux conditions when there are an infinite number of stages in the column.

In the *ternary separations* ( $N_c = 3$ ) considered here we first compute the  $(N_c - 1) = 2$  roots from the feed equation (Eq. 2). This gives  $\theta_A$  and  $\theta_B$ , which are the same for all the configurations. The root to be used in Eq. 1 depends on the split between the components and thus on the configurations considered. If we have a sharp A/BC split as for the DS configurations, then we use  $\theta_A$  and if we have a sharp AB/C split as for the IS configurations, then we use  $\theta_B$  in Eq. 1.

For the special case of a *binary separation* with components  $i$  and  $j$  the minimum vapor flow rate at the top of the column ( $V_{T,\min}$ ) for infinite number of stages can be calculated by using King's formula<sup>9</sup>

$$V_{T,\min} = \frac{r_{i,D} - \alpha_{ij}r_{j,D}}{\alpha_{ij} - 1} F + D \quad (3)$$

Here  $r_{i,D}$  and  $r_{j,D}$  are the recoveries of components  $i$  and  $j$  in the distillate, where the recovery of component  $i$  is defined as  $r_{i,D} = x_{i,D}D/z_iF$ . For a liquid feed the vapor flow rate at the top of the column equals the vapor flow rate at the bottom ( $V_{B,\min}$ ) and for a sharp split we have  $r_{i,D} = 1$  and  $r_{j,D} = 0$ . The minimum vapor flow rate for a binary sharp split with liquid feed is then

$$V_{T,\min} = \frac{1}{\alpha_{ij} - 1} F + D \quad (4)$$

For the ternary separation of ABC the relative volatilities of interest are  $\alpha_{AC}$  and  $\alpha_{BC}$ . For the binary AB and BC separations the relative volatilities of interest are  $\alpha_{AB} = \alpha_{AC}/\alpha_{BC}$  and  $\alpha_{BC}$ . If the relative volatilities then varies with pressure different relative volatilities should be used in the HP and LP column. In the  $V_{\min}$  equations we use the notation  $\alpha_{AB}$  or  $\alpha_{BC}$  to indicate that the relative volatilities are actually at different pressure levels.

### Minimum vapor flow rate for multieffect arrangements

The minimum vapor flow required for the multieffect configurations in Figures 2–4 can be found using the shortcut equations described above. It should be noted that when assuming constant relative volatility independent of pressure the multieffect configurations with the same split type have the same minimum vapor flow requirements (that is, DSF = DSB, ISF = ISB, and PF = PB). However, if the relative volatility is assumed to be a function of the pressures (and therefore temperatures) in the columns then the relative volatility in the HP and LP columns are different. The  $V_{\min}$  equations remain the same, but using different volatilities for the HP and LP columns will give different minimum vapor flow rates for same-split configurations, that is, DSF  $\neq$  DSB, ISF  $\neq$  ISB, and PF  $\neq$  PB.

With the assumptions of liquid flows, we have from Eqs. 1 and 4 that the minimum vapor flow rate for the individual

columns in the direct-split arrangements DSF and DSB in Figure 2 are

$$V_{\min}^{\text{CD1}} = \frac{\alpha_{AC}z_A}{\alpha_{AC} - \theta_A} F \quad (5)$$

$$V_{\min}^{\text{CD2}} = \frac{F}{\alpha'_{BC} - 1} (z_B + z_C) + \frac{z_B}{z_B + z_C} \quad (6)$$

The required minimum vapor flow rate for the multieffect integrated direct split configurations is equal to the highest vapor flow rate requirement in the individual columns, that is

$$V_{\min,DSF} = V_{\min,DSB} = \max\{V_{\min}^{\text{CD1}}, V_{\min}^{\text{CD2}}\} \quad (7)$$

To compare, for the nonintegrated direct split configuration (Figure 1a) the minimum vapor flow rate is the sum of the required vapor rates in each column

$$V_{\min,DS} = V_{\min}^{\text{CD1}} + V_{\min}^{\text{CD2}} \quad (8)$$

For the indirect-split arrangements ISF and ISB (Figure 3) the vapor flow rate for the individual columns is expressed as

$$V_{\min}^{\text{CI1}} = \left( \frac{\alpha_{AC}z_A}{\alpha_{AC} - \theta_B} + \frac{\alpha_{BC}z_B}{\alpha_{BC} - \theta_B} \right) F \quad (9)$$

$$V_{\min(q=1)}^{\text{CI2}} = \frac{F}{\alpha'_{AB} - 1} (z_A + z_B) + z_A F \quad (10)$$

For the multieffect integrated indirect split configurations with forward and backward integration the minimum vapor flow rate required is then the maximum of the two flow rates in the individual columns

$$V_{\min,ISF} = V_{\min,ISB} = \max\{V_{\min}^{\text{CI1}}, V_{\min(q=1)}^{\text{CI2}}\} \quad (11)$$

To compare with the nonintegrated arrangement (Figure 1b) we note that here it is better to partially condense the vapor from the first column so the feed to the second column is vapor ( $q = 0$ ). We have

$$V_{\min(q=0)}^{\text{CI2}} = \frac{F}{\alpha'_{AB} - 1} (z_A + z_B) \quad (12)$$

So the minimum vapor flow rate for the nonintegrated indirect split configuration (Figure 1b) is then

$$V_{\min,IS} = V_{\min}^{\text{CI1}} + V_{\min(q=0)}^{\text{CI2}} \quad (13)$$

We next consider the *prefractionator arrangement* (Figure 4). In the prefractionator column (C1) there is a sharp split between the lightest (A) and the heaviest (C) component (A/C), that is,  $x_{A,D}D = z_A F$  and  $x_{C,D} = 0$  in Eq. 1. However, from Eq. 1 the minimum vapor flow rate will depend on the amount of the middle (B) component in the distillate, as expressed by

$x_{B,D}$ . This can alternatively be expressed in terms of the *product split* from the prefractionator column

$$\eta \triangleq \frac{D^{C1}}{F} \quad (14)$$

Note that  $x_{B,D}D = F(\eta - z_A)$  so from Eq. 1  $V_{\min}$  will depend linearly on  $\eta$ .

Furthermore, Eq. 2 gives two possible Underwood roots ( $\theta_A$  and  $\theta_B$ ) and the two corresponding values of  $V_{\min}$  are from Eq. 1

$$V_{\min(\theta=\theta_A)}^{C1} = \left( \frac{\alpha_{AC}z_A}{\alpha_{AC} - \theta_A} + \frac{\alpha_{BC}(\eta - z_A)}{\alpha_{BC} - \theta_A} \right) F \quad (15)$$

$$V_{\min(\theta=\theta_B)}^{C1} = \left( \frac{\alpha_{AC}z_A}{\alpha_{AC} - \theta_B} + \frac{\alpha_{BC}(\eta - z_A)}{\alpha_{BC} - \theta_B} \right) F \quad (16)$$

Note the linear dependency on  $\eta$ . In the prefractionator the minimum vapor flow rate as a function of the recovery  $\eta$  is the maximum of these two<sup>7</sup>

$$V_{\min}^{C1}(\eta) = \max[V_{\min(\theta=\theta_A)}^{C1}, V_{\min(\theta=\theta_B)}^{C1}] \quad (17)$$

This gives a V-shaped curve as a function of  $\eta$  and the minimum vapor flow rate in the prefractionator column occurs at a specific value of  $\eta_{preferred}$ , called “the preferred split.”

However, to find the optimal value of  $\eta$  for the multieffect arrangement we also have to consider the vapor flow required in the main column. The two sections of the main column performs sharp binary separations and from Eq. 4 the minimum vapor flow rate in the upper section (C21) of the main column is

$$V_{\min}^{C21}(\eta) = \frac{\eta F}{\alpha'_{AB} - 1} + z_A F \quad (18)$$

and in the lower section (C22)

$$V_{\min}^{C22}(\eta) = \left[ \frac{1 - \eta}{\alpha'_{BC} - 1} + (1 - \eta - z_C) \right] F \quad (19)$$

Note again the linear dependency on  $\eta$ .

Because column sections C21 and C22 are connected the minimum vapor flow rate in the main column is the maximum of the two. The minimum flow rate of the integrated prefractionator arrangement (Figure 4) is the maximum of the main column and the prefractionator and by adjusting  $\eta$  we have

$$V_{\min,PF} = V_{\min,PB} = \min_{\eta} \{ \max[V_{\min}^{C1}(\eta), V_{\min}^{C21}(\eta), V_{\min}^{C22}(\eta)] \} \quad (20)$$

The “optimum” recovery  $\eta$  occurs at the lowest minimum vapor flow rate for the system.

To compare, for the *nonintegrated prefractionator* arrangement (Figure 1c) we have

$$V_{\min,P} = \min_{\eta} \{ V_{\min}^{C1}(\eta) + \max[V_{\min}^{C21}(\eta), V_{\min}^{C22}(\eta)] \} \quad (21)$$

However, here it turns out that the minimum vapor flow requirement is always at the “preferred split” ( $\eta = \eta_{preferred}$ ). For the integrated prefractionator arrangements the preferred split will be optimal in only some cases (see below).

## Visualizing the Vapor Flow Requirements in a $V[b]_{\min}$ Diagram

From the above equations we see that a plot of  $V_{\min}$  against the prefractionator split  $\eta = D^{C1}/F$  will result in straight lines. This observation is the basis for the proposed  $V_{\min}$  diagram previously used by Halvorsen and Skogestad<sup>10</sup> for the Petlyuk column. In this section, we show how to draw the diagrams for the multieffect arrangements. Their use is discussed in subsequent sections.

To draw the  $V_{\min}$  diagram in Figure 5 for the prefractionator column (C1) we have to identify five points  $[\eta, V_{T,\min}]$ . For sharp splits and liquid feeds these are obtained from the equations above (see also Halvorsen and Skogestad<sup>10</sup>)

$$P_{AB}: \left( z_A, \frac{\alpha_{AC}z_A}{\alpha_{AC} - \theta_A} \right) \quad (22)$$

$$P_{BC}: \left( z_A + z_B, \frac{\alpha_{AC}z_A}{\alpha_{AC} - \theta_B} + \frac{\alpha_{BC}z_B}{\alpha_{BC} - \theta_B} \right) \quad (23)$$

$$P_{AC}: \left[ \eta_{preferred} \frac{\alpha_{AC}z_A}{\alpha_{AC} - \theta_B} + \frac{\alpha_{BC}(\eta_{preferred} - z_A)}{\alpha_{BC} - \theta_B} \right] \quad (24)$$

Point  $P_{AC}$  is at the “preferred” split where

$$\eta_{preferred} = z_A - \frac{\alpha_{AC}z_A(\alpha_{BC} - \theta_A)(\alpha_{BC} - \theta_B)}{\alpha_{BC}(\alpha_{AC} - \theta_A)(\alpha_{AC} - \theta_B)} \quad (25)$$

Finally, we have points  $P_0$  and  $P_1$ . These are actually not used in this paper, but they complete the diagram for the prefractionator

$$P_0: = [0, 0] \quad (26)$$

$$P_1: = [1, (1 - q)] \quad (27)$$

In the  $V_{\min}$  diagram (Figure 5) the peak  $P_{A/B}$  is the minimum vapor flow for a sharp split between A/B with C present (A/BC) and the peak  $P_{B/C}$  gives the minimum vapor flow for a sharp B/C split with A present (AB/C). The curve between the points  $P_{AB}-P_{AC}-P_{BC}$  gives the minimum vapor flow rate for sharp split between A and C for different recoveries of B in the distillate from the prefractionator. Along and above this line the split between A and C is sharp, with B distributed between the top and bottom product. The “preferred split” at point  $P_{AC}$  gives the minimum vapor flow rate for a sharp split between the lightest component (A) and the heaviest component (C) in the prefractionator. Note that below the dotted line where  $D = V_T$



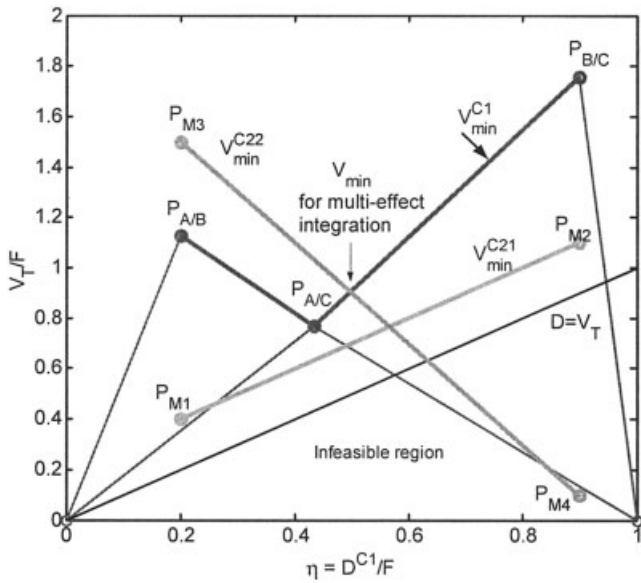


Figure 6. Extended  $V_{\min}$  diagram for the multieffect prefractionator arrangement in Figure 4 (Case 1).

the separation in the prefractionator is infeasible because we must have that  $V_T < D$ .

For the Petlyuk column the minimum vapor flow rate is the highest of the peaks in the  $V_{\min}$  diagram,<sup>10</sup> that is

$$V_{\min, \text{Petlyuk}} = \max[V_{A/B}, V_{B/C}] \quad (28)$$

where  $V_{A/B}$  and  $V_{B/C}$  correspond to the points  $P_{A/B}$  and  $P_{B/C}$ , respectively, in Figure 5.

The diagram in Figure 5 corresponds to the prefractionator column (C1) in Figure 4. In Figure 6 the  $V_{\min}$  diagram is extended to the entire multieffect arrangement by including the relationships for the minimum vapor flow rate in the two sections of the main column.

The additional four coordinates for the extended diagram are for the main column sections C21 and C22. They are found from the minimum vapor flow rate expression (Eq. 4) for binary separation with sharp splits and liquid feed.

The two points  $[\eta, V_{T, \min}]$  for the upper section of the main column (C21) are

$$P_{M1}: \left( z_A, \frac{z_A}{\alpha'_{AB} - 1} + z_A \right) \quad (29)$$

$$P_{M2}: \left( z_A + z_B, \frac{z_A + z_B}{\alpha'_{AB} - 1} + z_A \right) \quad (30)$$

and the two points for the lower section of the main column (C22) are

$$P_{M3}: \left( z_A, \frac{z_B + z_C}{\alpha'_{BC} - 1} + z_B \right) \quad (31)$$

$$P_{M4}: \left( z_A + z_B, \frac{z_C}{\alpha'_{BC} - 1} \right) \quad (32)$$

It should be noted that in Figure 6 the lines for  $V^{C21}$  and  $V^{C22}$  go from  $\eta = z_A$  (points  $P_{M1}$  and  $P_{M3}$ ) to  $\eta = z_A + z_B$  (points  $P_{M2}$  and  $P_{M4}$ ). To the left of points  $P_{M1}$  and  $P_{M3}$  there is no B present in the feed to the upper part of the main column so all of B goes to the lower part of the main column. To the right of points  $P_{M2}$  and  $P_{M4}$  all of B is fed to the upper part of the main column and no B goes to the lower part.

### Using the $V_{\min}$ Diagram for the Multieffect Prefractionator Column

In the multieffect prefractionator arrangement in Figure 4 the vapor flow in all three column sections must be equal. It then follows that the minimum vapor flow for a given recovery of component B in the prefractionator (given value of  $\eta = D^{C1}/F$ ) is the maximum of the minimum flow rates in the three sections. The value of  $\eta$  should be adjusted such that  $V_{\min}$  is minimized. The minimum vapor flow for the multieffect prefractionator arrangement is then

$$V_{\min, PF} = V_{\min, PB} = \min_{\eta} \{ \max[V_{\min}^{C1}(\eta), V_{\min}^{C21}(\eta), V_{\min}^{C22}(\eta)] \} \quad (33)$$

Importantly, this value can easily be found using the  $V_{\min}$  diagram in Figure 6, as is further illustrated in Table 1.

When we require sharp split the points  $P_{A/B}$ ,  $P_{A/C}$ , and  $P_{B/C}$  span the minimum vapor flow rate for the prefractionator column (shown in bold). The points for the main column are shown as  $P_{M1}$ – $P_{M2}$  (C21) and  $P_{M3}$ – $P_{M4}$  (C22). For the specific case in Figure 6 the minimum vapor flow as a function of  $\eta$ ,  $V_{\min, PF}(\eta)$ , follows the  $V_{\min}^{C22}$  line from the point  $P_{M3}$  and down to the crossing with the  $V_{\min}^{C1}$  line and then goes up to the point  $P_{B/C}$ . The minimum vapor flow rate for the overall multieffect integrated prefractionator arrangement is then where the  $V^{C22}$  and  $V^{C1}$  lines cross (indicated as  $V_{\min}$  in the figure).

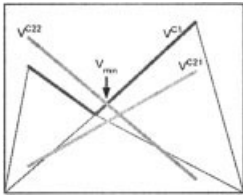
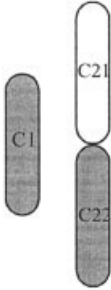
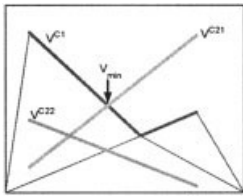

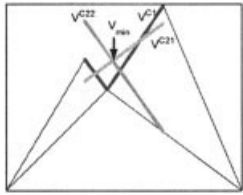
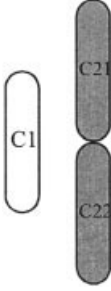
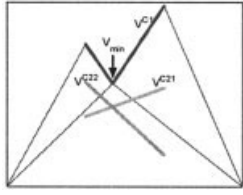
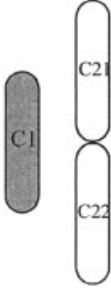
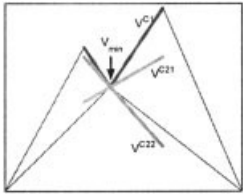
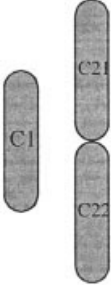
The case shown in Figure 6 is referred to as Case 1. More generally, we have the following five possibilities for the multieffect prefractionator arrangements:

- Case 1: Lines for  $V^{C22}$  and  $V^{C1}$  cross at optimum:  $V^{C1} = V^{C22} > V^{C21}$
- Case 2: Lines for  $V^{C21}$  and  $V^{C1}$  cross at optimum:  $V^{C1} = V^{C21} > V^{C22}$
- Case 3: Lines for  $V^{C21}$  and  $V^{C22}$  cross at optimum:  $V^{C21} = V^{C22} > V^{C1}$
- Case 4: Optimum at “preferred split”; no lines cross:  $V^{C1} > V^{C21}$  and  $V^{C22}$
- Case 5: All lines cross in the same point at optimum:  $V^{C1} = V^{C21} = V^{C22}$

The left column in Table 1 shows the  $V_{\min}$  diagrams for these different cases. We can also use the information from the  $V_{\min}$  diagram to find the column sections that receive excess vapor (“unbalanced sections”). The column sections receiving excess vapor are shown in white in the middle column in Table 1. The “limiting” column sections, which operate at minimum flows, are shown in gray.

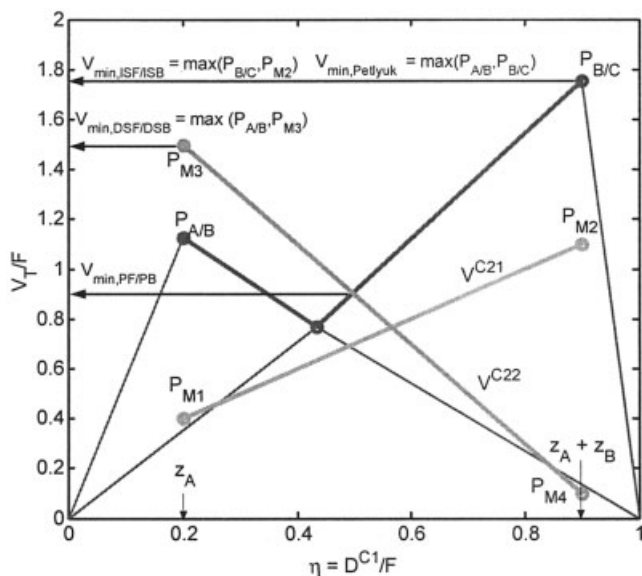
Except for Case 5 there will always be an excess (or “unbalance”) of vapor flow requirement in some column section. The last column of Table 1 summarizes the design or operational options that are available for the different classes. Note that the options available can differ depending on the arrangement, PF or PB, used. The difference occurs because for the PF

**Table 1. Possible  $V_{min}$  Diagrams for Multieffect Prefractionator**

$V_{min}$ Diagram	Limiting Column Sections	Possible Use of Excess Vapor
<p>Case 1 (<math>V^{C1} = V^{C22} &gt; V^{C21}</math>)</p> 		<p><u>PF</u></p> <ul style="list-style-type: none"> <li>a) Intermediate condenser between C22 and C21.</li> <li>b) Overpurify C21 product.</li> <li>c) Vapor sidestream product.</li> </ul>
<p>Case 2 (<math>V^{C1} = V^{C21} &gt; V^{C22}</math>)</p> 		<p><u>PF</u></p> <ul style="list-style-type: none"> <li>a) Overpurify C22 product.</li> </ul> <p><u>PB</u></p> <ul style="list-style-type: none"> <li>a) Intermediate reboiler between C22 and C21.</li> <li>b) Overpurify C22 product.</li> </ul>
<p>Case 3 (<math>V^{C21} = V^{C22} &gt; V^{C1}</math>)</p> 		<p><u>PF</u></p> <p>Not common, unless <math>\alpha</math> increases with pressures.</p> <p><u>PB</u></p> <p>Overpurification in C1 is possible, but not important for final products.</p> <ul style="list-style-type: none"> <li>a) Use shorter column (C1).</li> <li>b) Intermediate condenser at top of C21.</li> </ul>
<p>Case 4 (<math>V^{C21} = V^{C22} &lt; V^{C1}</math>)</p> 		<p><u>PF</u></p> <ul style="list-style-type: none"> <li>a) Intermediate condenser between C22 and C21, or between C1 and C22.</li> <li>b) Overpurify products from main column.</li> <li>c) Vapor sidestream product.</li> <li>d) Shorter column sections (C21 and C22).</li> </ul> <p><u>PB</u></p> <p>Not common, unless <math>\alpha</math> increases with pressures.</p>
<p>Case 5 (<math>V^{C1} = V^{C1} = V^{C22}</math>)</p> 		<p>All column sections are balanced. No special measures needed.</p>

Note: White sections receive excess vapor, that is, are overfluxed.





**Figure 7. Use of  $V_{\min}$  diagram to find minimum vapor flow rate for various column arrangements, with relative volatility independent of pressure.**

arrangement the heat input is to the prefractionator column (C1), whereas for the PB arrangement the heat input is to the lower section of the main column (C2).

### $V_{\min}$ Diagram for Other Column Configurations

The  $V_{\min}$  diagram can also be used to find the minimum vapor flow rate of other column arrangements. This is shown in Figure 7 for the following multieffect arrangements:

- Direct split with forward and backward integration (DSF/DSB).
- Indirect split with forward and backward integration (ISF/ISB).

The minimum vapor flow rate for the DSF/DSB arrangement in Figure 7 is the maximum of the two points  $P_{A/B}$  and  $P_{M3}$ . For the ISF/ISB arrangement the minimum vapor flow rate is the maximum of the two points  $P_{B/C}$  and  $P_{M2}$ . The difference between these points will also indicate how the columns are unbalanced. It is easy to see from the diagram which of the integrated DS or IS arrangement has the lowest energy demand.

We have here assumed no difference in the relative volatilities for the forward and backward integrated cases, so that  $V_{DSF} = V_{DSB}$  and  $V_{ISF} = V_{ISB}$ . If the relative volatilities are expected to vary with pressure then different relative volatilities for the HP and the LP column should be used (this will give different  $V_{\min}$  diagrams for the different same split arrangements).

The  $V_{\min}$  diagram can also be used to find the minimum vapor flow rate for the nonintegrated single pressure direct split (DS) and indirect split (IS) arrangements. The minimum vapor flow rate for direct split is the sum of ( $P_{A/B} + P_{M3}$ ) and for the indirect split (IS) the sum of ( $P_{B/C} + P_{M2}$ ). Finally, minimum vapor flow rate for the Petlyuk column is, as mentioned earlier, the maximum of the peaks ( $P_{A/B}, P_{B/C}$ ).

In summary we then have, with reference to Figure 7 (see Table 1):

DS (nonintegrated)	$V_{\min} = P_{A/B} + P_{M3}$
IS (nonintegrated)	$V_{\min} = P_{B/C} + P_{M2}$
DSF/DSB	$V_{\min} = \max(P_{A/B}, P_{M3})$
ISF/ISB	$V_{\min} = \max(P_{B/C}, P_{M2})$
Petlyuk (nonintegrated)	$V_{\min} = \max(P_{A/B}, P_{B/C})$
PF/PB	$V_{\min} = \min_{\eta}[\max(V_{\min}^{C1}, V_{\min}^{C21}, V_{\min}^{C22})]$

The above summary, together with Figure 7, provides the main contribution of this article.

The  $V_{\min}$  diagram in Figure 7 can thus be used as a screening method to quickly determine whether multieffect distillation (especially that with a prefractionator) should be investigated further.

From the shape of the  $V_{\min}$  diagram it can be seen that, with the constant relative volatility assumption (independent of pressure), the multieffect prefractionator arrangement (PF/PB) will always be better than the other multieffect arrangements considered here. It will also always be better than the nonintegrated arrangements, including the Petlyuk column. This is further confirmed by the data in Table 2.

From the diagram one can also find the optimal split  $D^{C1}/F$  in the prefractionator column. For the Petlyuk arrangement the optimal is at the preferred split, corresponding to point  $P_{A/C}$  in Figure 5. For most cases of the integrated prefractionator arrangement, however, the optimal recovery does not coincide with the preferred split of the Petlyuk column. For the integrated prefractionator the optimal split usually lies between the preferred split and the “balanced split” defined for a nonintegrated prefractionator arrangement.<sup>8</sup>

## Case Studies

### Minimum vapor flow rate using shortcut equations

Table 2 summarizes some results for different distillation arrangements when calculating the minimum vapor flow rate using the shortcut equations described earlier, assuming constant relative volatility independent of pressure, liquid feed, constant molar flows, and sharp splits.

The minimum energy requirement ( $V_{\min}$ ) is expressed as the percentage improvement compared to the best of the nonintegrated direct (DS) or indirect split (IS) arrangements. The conventional non-heat-integrated and multieffect arrangements are considered, as well as the Petlyuk arrangement. The results are presented for five different feeds (equimolar feed, feeds with large amount of the intermediate component, feed with a small amount of the intermediate component, and a feed with large amount of the lightest component) and five different relative volatilities. The relative volatilities considered for the different feed cases are: equal difficulty between A/B and B/C, difficult A/B, difficult B/C, difficult A/B and B/C, and easy A/B and B/C.

From these results the following general observations were made, in terms of “*first-law*” energy requirements:

- The integrated prefractionator arrangements are always better than the other arrangements.
- The highest energy savings for the integrated prefractionator arrangements occur when there is a high concentration of the middle component in the feed. The percentage savings for some of the cases exceed 70%. The highest savings, when there is a high concentration of B, is when the relative volatilities are more or less “balanced” (that is, the same level of difficulty between the A/B and B/C separation).

**Table 2. Percentage Energy Savings Compared with the Best of the Conventional DS or IS (without Multieffect Heat Integration), Assuming  $\alpha$  Constant with Pressure**

$z_F$	Column Arrangement	$\alpha = [4\ 2\ 1]$	$\alpha = [5\ 4.5\ 1]$	$\alpha = [5\ 1.5\ 1]$	$\alpha = [2\ 1.5\ 1]$	$\alpha = [10\ 5\ 1]$
1/3	DS	-1.94	0.00	-4.98	0.00	-0.28
	IS	0.00	-0.51	0.00	0.00	0.00
	Petlyuk	32.80	7.59	12.76	39.54	32.71
1/3	DSF/DSB	47.26	7.59	25.56	39.54	32.71
	ISF/ISB	32.80	8.21	12.76	44.65	34.03
	PF/PB	<b>61.73</b>	<b>37.44</b>	<b>47.41</b>	<b>59.06</b>	<b>50.05</b>
0.10	DS	-0.09	0.00	-0.23	0.00	-0.01
	IS	0.00	-0.03	0.00	0.00	0.00
	Petlyuk	32.99	11.39	12.43	47.37	44.23
0.10	DSF/DSB	37.69	11.39	16.20	47.34	49.62
	ISF/ISB	32.99	11.63	12.43	49.02	44.23
	PF/PB	<b>65.55</b>	<b>52.83</b>	<b>54.54</b>	<b>71.71</b>	<b>71.80</b>
0.20	DS	0.00	0.00	-1.06	0.00	0.00
	IS	-0.66	-0.49	0.00	-2.11	-0.52
	Petlyuk	33.40	8.50	13.41	40.03	37.72
0.20	DSF/DSB	48.91	8.50	25.70	40.03	37.72
	ISF/ISB	33.40	8.89	13.41	43.12	38.53
	PF/PB	<b>64.43</b>	<b>42.87</b>	<b>52.40</b>	<b>62.01</b>	<b>57.39</b>
0.45	DS	-6.25	0.00	-17.42	0.00	-0.78
	IS	0.00	-1.38	0.00	0.00	0.00
	Petlyuk	34.38	4.53	14.19	34.78	18.39
0.45	DSF/DSB	34.38	4.53	27.74	34.78	18.39
	ISF/ISB	34.38	4.90	14.19	39.13	19.26
	PF/PB	<b>42.58</b>	<b>18.40</b>	<b>37.29</b>	<b>45.65</b>	<b>26.45</b>
0.80	DS	0.00	0.00	0.00	0.00	0.00
	IS	-10.25	-2.14	-3.75	-17.43	-4.07
	Petlyuk	14.96	1.73	19.04	12.45	8.10
0.10	DSF/DSB	14.96	1.73	29.55	12.45	8.10
	ISF/ISB	15.23	1.77	19.04	12.86	8.18
	PF/PB	<b>19.92</b>	<b>10.78</b>	<b>32.34</b>	<b>19.68</b>	<b>13.27</b>

- The lowest energy savings for all arrangements are when the feed contains a lot of the light component (A), or small amounts of heavy component (C), or small amounts of the middle component.
- There is generally a large difference between the integrated prefractionator arrangements and the Petlyuk arrangement, which is the best nonintegrated arrangement.<sup>6</sup> The improvement ranges from about 5 to 47%, depending on the difficulty of separation and feed composition. The lowest savings are when there is a large amount of light component in the feed and the highest savings are when there is a high amount of the middle component in the feed.

For the calculations in Table 2 the same relative volatility has been used for both columns. This is the simplest assumption and it is in agreement with the assumption of equal heat of vaporization made when assuming constant molar flows. For real mixtures, the relative volatility is usually reduced when we increase the pressure, but this is not always the case (such as a mixture of methanol and ethyl acetate).

### Analysis of a BTX separation using $V_{min}$ diagrams

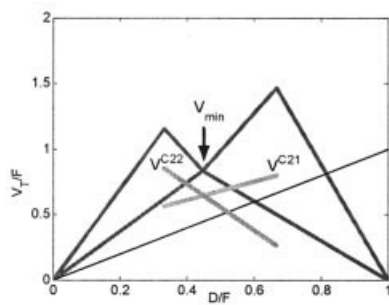
The  $V_{min}$  diagram is here used to analyze a mixture of benzene, toluene, and *m*-xylene (BTX). The relative volatilities for this mixture are given in Table 3. In this example we have included pressure variations in the relative volatility, which is important for practical considerations. The relative volatilities used have been calculated at HP = 6 bar and LP = 1 bar, using a commercial simulation package. The pressure of 6 bar in the HP column has been selected because it gives a sufficient temperature driving force between the multieffect integrated columns. For the main column the relative volatilities given are for the upper section of the main column  $\alpha_{AB}$  and for the lower section of the main column  $\alpha_{BC}$ .

Figure 8 shows the  $V_{min}$  diagrams for this mixture using the forward-integrated prefractionator arrangement (PF) at two different feed compositions:  $z_F = [1/3\ 1/3\ 1/3]$  and  $z_F = [0.15\ 0.7\ 0.15]$ . Figure 9 shows the same mixture and feed compositions, but for the backward-integrated arrangement (PB). Note that the reason for the difference between the PF and PB arrange-

**Table 3. Relative Volatilities for BTX Mixtures**

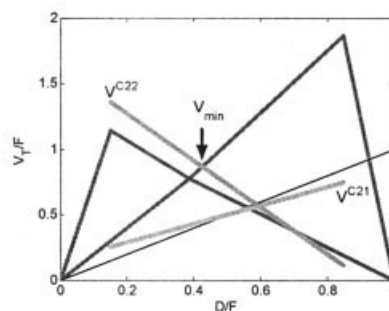
	Forward Integration (PF)			Backward Integration (PB)		
	Prefractionator (LP)	Main Column (HP)		Prefractionator (HP)	Main Column (LP)	
	C1	C21	C22	C1 (HP)	C21	C22
Benzene	3.58	2.43		5.57	1.90	1.88
Toluene	1.88	1.00	2.29	2.29	1.00	1.00
<i>m</i> -Xylene	1.00		1.00	1.00		

a)  $z_F = [1/3 \ 1/3 \ 1/3]$  - Case 4-PF



$$V_{\min}/F = 0.835$$

b)  $z_F = [0.15 \ 0.7 \ 0.15]$  - Case 1-PF



$$V_{\min}/F = 0.865$$

Figure 8.  $V_{\min}$  diagram for BTX mixture using PF arrangement ( $\alpha$  depends on pressure).

ment is the dependency of the relative volatility on the pressure. For the PF system the high-pressure column is the prefractionator, whereas for the PB system the high-pressure column is the main column. The relative volatilities used reflect this difference.

It can be seen from Figure 8a, that at equimolar feed the minimum energy demand in the prefractionator column is higher than the minimum energy demand in both sections of the main column (case 4 in Table 1). The main column will then have to run at a higher reflux than necessary, with the result that the column can be made shorter (arising from the trade-off between reflux and number of stages). Alternatively the products in the main column can be overpurified.

In the case of the feed with the high concentration of the middle component the energy demand in the prefractionator and the lower section of the main column is balanced (see Figure 8b). The energy demand in the upper section of the main column is less than that of the other two sections (case 1 in Table 1). In this case there are two options: to use a lesser number of stages in the upper section (and higher reflux) or to use an intermediate condenser between the upper and lower section of the main column. A third option would be to overpurify the light component.

For the equimolar feed using the PB arrangement the minimum energy demand in the main column is higher than that in

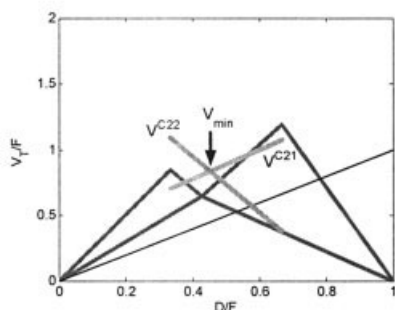
the prefractionator (case 3 in Table 1; see Figure 9a). This is a backward-integrated scheme so the main column is used to boil the prefractionator column. There are two options for balancing the columns: to condense some of the vapor at the top of the main column or to run the prefractionator column at a higher reflux and use fewer stages.

For the feed with the high concentration of the middle component the upper section of the main column has a lower vapor flow demand and we have a case in Table 1. We cannot install an intermediate condenser between the two column sections and the prefractionator requires a higher vapor flow than does the upper section. The option will be to reduce the number of stages in the upper section while running at the higher reflux rate. Another option would be to overpurify the light product.

## Conclusions

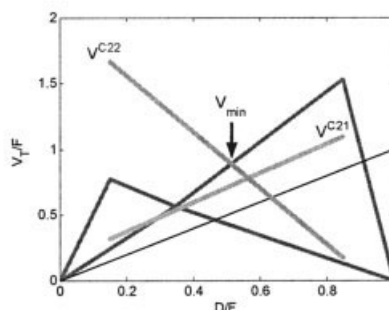
Shortcut equations for minimum vapor flow in ternary multieffect distillation systems have been presented. Using these shortcut equations it was shown that the multieffect prefractionator arrangement is always better than the other multieffect

a)  $z_F = [1/3 \ 1/3 \ 1/3]$  - Case 3-PB



$$V_{\min}/F = 0.855$$

b)  $z_F = [0.15 \ 0.7 \ 0.15]$  - Case 1-PB



$$V_{\min}/F = 0.871$$

Figure 9.  $V_{\min}$  diagram for BTX Mixture using PB arrangement ( $\alpha$  depends on pressure).

arrangements considered, when assuming constant relative volatility, constant molar flows, liquid feeds, and sharp splits.

The energy saving of the multieffect prefractionator was also shown in a  $V_{\min}$  diagram. For a prefractionator or Petlyuk column a  $V_{\min}$  diagram can be plotted to show the minimum vapor flow rate as a function of the distillate flow rate, when there are infinite number of stages in the columns. For a ternary mixture it has been shown how this diagram can be extended to include heat-integrated multieffect arrangements. It has been shown how the  $V_{\min}$  diagram then can be used to find the minimum vapor flow rate for all conventional nonintegrated and multieffect integrated arrangements. Figure 7 summarizes these results in a single  $V_{\min}$  diagram.

From both the shortcut equations and the  $V_{\min}$  diagram it was shown that the multieffect prefractionator has the lowest energy consumption compared with the other arrangements studied.

The calculation of  $V_{\min}$  assumes infinite number of stages, however, this is not in itself an important limitation since the actual value of  $V$  is usually close to  $V_{\min}$ . Thus,  $V_{\min}$  provides a good target for comparing energy usage for alternative arrangements. Of course, when selecting the best arrangements one must also consider other factors such as capital costs, operability and control, product flexibility, available utilities, and other often case-to-case specific requirements.

Herein the formulas for the points in the  $V_{\min}$  diagrams have been given for sharp splits but they can easily be extended to nonsharp splits.<sup>11</sup> The lines in the  $V_{\min}$  diagram will remain straight, but they will be shifted slightly downward, although usually not much because  $V_{\min}$  is proportional to the purity:  $V_{\min}$  for 98% purity is 98% of that for sharp separation splits. The main effect of purity is on the required number of stages, which increases in proportion to the log of the impurity.<sup>12</sup>

The main assumptions foundational to this study are those of constant relative volatility and constant molar flows. For real mixtures similar diagrams may be generated by simulation.

## Literature Cited

1. Hewitt G, Quarini J, Morell M. More efficient distillation. *Chem Eng.* 1999;Oct. 21.
2. Cheng HC, Luyben W. Heat-integrated distillation columns for ternary separations. *Ind Eng Chem Process Des Dev.* 1985;24:707-713.
3. Emtir M, Rév E, Fonyó Z. Rigorous simulation of energy integrated and thermally coupled distillation schemes for ternary mixture. *Appl Therm Eng.* 2001;21:1299-1317.
4. Rév E, Emtir M, Sztikai Z, Mizsey P, Fonyó Z. Energy savings of integrated and coupled distillation systems. *Comput Chem Eng.* 2001; 25:119-140.
5. Carlberg NA, Westerberg AW. Temperature-heat diagrams for complex columns. 3. Underwood's method for the Petlyuk configuration. *Ind Eng Chem Res.* 1989;28:1386-1397.
6. Halvorsen IJ. *Minimum Energy Requirements in Complex Distillation Arrangements.* PhD Thesis. Trondheim, Norway: Norwegian University of Science and Technology; 2001.
7. Fidkowski Z, Krolikowski L. Thermally coupled system of distillation columns: Optimization procedure. *AIChE J.* 1986;32:537-546.
8. Christiansen AC. *Studies on Optimal Design and Operation of Integrated Distillation Arrangements.* PhD Thesis. Trondheim, Norway: Norwegian University of Science and Technology; 1997.
9. King CJ. *Separation Processes.* 2nd Edition. New York, NY: McGraw-Hill; 1980.
10. Halvorsen IJ, Skogestad S. Minimum energy consumption in multi-component distillation. 1.  $V_{\min}$  diagram for a two product column. *Ind Eng Chem Res.* 2003a;42:596-604.
11. Halvorsen IJ, Skogestad S. Minimum energy consumption in multi-component distillation. 2. Three product Petlyuk arrangements. *Ind Eng Chem Res.* 2003b;42:605-615.
12. Skogestad S. Dynamics and control of distillation columns. *Trans IChemE.* 1997;75A:539-562.

Manuscript received Feb. 20, 2004, and revision received Oct. 22, 2004